Chemistry & Biology
Article

A Small-Molecule Inducer of the Antioxidant Response Element

Wooyoung Hur,[1] Zheng Sun,[2] Tao Jiang,[2] Daniel E. Mason,[3] Eric C. Peters,[3] Donna D. Zhang,[2] Hendrik Luesch,[4,*] Peter G. Schultz,[1,3,*] and Nathanael S. Gray[5,*]
[1]Department of Chemistry, The Scripps Research Institute, La Jolla, CA 92037, USA
[2]Department of Pharmacology and Toxicology, College of Pharmacy, University of Arizona, Tucson, AZ 85721, USA
[3]Genomics Institute of the Novartis Research Foundation, San Diego, CA 92121, USA
[4]Department of Medicinal Chemistry, University of Florida, Gainesville, FL 32610, USA
[5]Department of Cancer Biology, Dana Farber Cancer Institute, Harvard Medical School, Boston, MA 02115 USA
*Correspondence: luesch@cop.ufl.edu (H.L.), schultz@scripps.edu (P.G.S.), Nathanael_Gray@dfci.harvard.edu (N.S.G.)
DOI 10.1016/j.chembiol.2010.03.013

SUMMARY

Eukaryotic cells counteract oxidative and other environmental stress through the activation of Nrf2, the transcription factor that controls the expression of a host of protective enzymes by binding to the antioxidant response element (ARE). The electrophilic molecules that are able to activate Nrf2 and its downstream target genes have demonstrated therapeutic potential in carcinogen-induced tumor models. Using a high-throughput cellular screen, we discovered a class of ARE activator, which we named AI-1, that activates Nrf2 by covalently modifying Keap1, the negative regulator of Nrf2. Biochemical studies indicated that modification of Cys151 of Keap1 by AI-1 disrupted the ability of Keap1 to serve as an adaptor for Cul3-Keap1 ubiquitin ligase complex, thereby causing stabilization and transcriptional activation of Nrf2. AI-1 and its biotinylated derivative are useful pharmacological probes for investigating the molecular details of the cellular antioxidant response.

INTRODUCTION

To survive in an aerobic environment, eukaryotic cells must protect essential cellular components from oxidative damage (Halliwell, 2007). The major defensive mechanisms that cells have developed to counteract oxidative and environmental stress involve the coordinated up-regulation of a group of enzymes that detoxify reactive species and restore cellular redox homeostasis. Classic phase 2 enzymes, such as glutathione *S*-transferase (GST) and NAD(P)H:quinone oxidoreductase 1 (NQO1), are an important group of cytoprotective enzymes, and their induction is controlled at the transcriptional level by a *cis*-acting enhancer sequence termed "antioxidant response element" (ARE) (Kensler et al., 2007; Wang et al., 2007; Wasserman and Fahl, 1997). A variety of naturally occurring and synthetic compounds are believed to mediate their therapeutic ability to protect against environmental carcinogens, aging, and neurodegeneration by stimulating the ARE pathway (Surh, 2003; van Muiswinkel and Kuiperij, 2005). Here, we report the discovery of a new class of synthetic, potent, small-molecule ARE inducer, which we named **AI-1**, that was identified using a high-throughput cell-based reporter gene assay. Using a cell-permeable biotin-derivatized analog and mass spectrometry, we have discovered that its molecular target is Kelch-like ECH-associated protein 1 (Keap1). In contrast to known ARE inducers that are highly reactive (isothiocyanates) or require metabolic activation (phenols), **AI-1** possesses an aromatic chloride that undergoes a nucleophilic aromatic substitution reaction with cysteine thiols of Keap1.

Nuclear factor E2–related factor 2 (Nrf2), a Cap 'n' Collar (CNC) type basic region-leucine zipper (bZIP) transcription factor, binds to the ARE sequence as a heterodimer with one of the small bZIP proteins, Mafs, and activates ARE-dependent transcription (Figure 1A). Nrf2 contains six functional domains that are conserved across species designated Neh1-6 (Nrf2-ECH homology1–6) domains (Figure 1B). The *N*-terminal Neh2 domain mediates binding with the cytosolic repressor of Nrf2 (Keap1) (Itoh et al., 1999). Neh4 and Neh5 are transactivation domains that bind cooperatively to CREB-binding protein (Katoh et al., 2001). Neh1 domain contains the CNC-type bZIP domain, enabling Nrf2 to form a heterodimer with the bZIP domain of small Maf proteins.

Nrf2 is negatively regulated by interaction with the 75 kDa cysteine-rich protein Keap1 (Dinkova-Kostova et al., 2005; Kobayashi and Yamamoto, 2006; Zhang, 2006). Keap1 has three main functional domains: an *N*-terminal Broad complex, Tramtrack, and Bric-a-brac (BTB) domain; a central intervening region (IVR); and a series of Kelch repeats located proximal to the C terminus (Figure 1B). The Kelch domain mediates binding with the Neh2 domain of Nrf2 (Padmanabhan et al., 2006), whereas the BTB domain mediates association with ubiquitin E3 ligase scaffold protein Cullin-3 (Cul3) (Zhang et al., 2004). Keap1 was initially thought to sequester Nrf2 in the cytoplasm by anchoring it to the actin cytoskeleton (Itoh et al., 1999). Later, it was found that Keap1 also functions as an adaptor protein for the Cul3-based E3 ubiquitin ligase that targets Nrf2 for ubiquitin conjugation and subsequent proteasomal degradation (Furukawa and Xiong, 2005; Kobayashi et al., 2004; Zhang et al., 2004). Two evolutionarily conserved motifs within the Neh2 domain (Tong et al., 2006), namely a DLG motif (formulated as

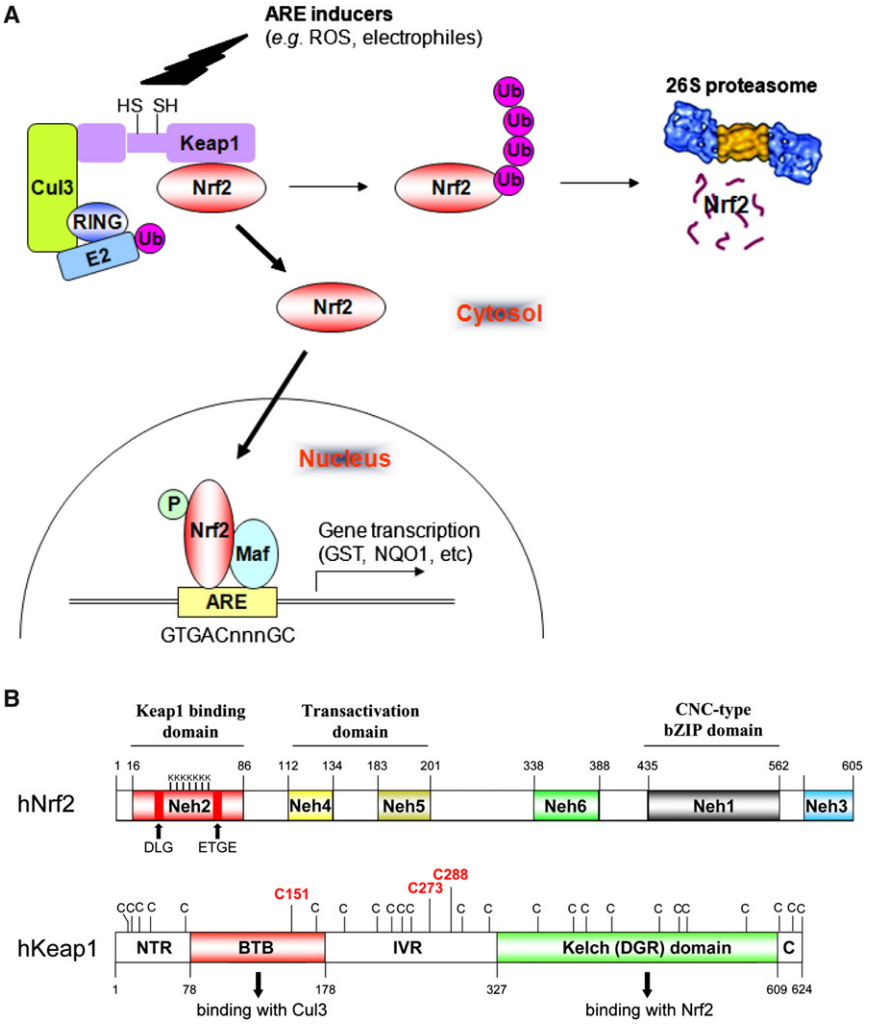

Figure 1. Current Model of the Keap1/Nrf2/ARE Pathway

(A) Under normal conditions, Nrf2 is negatively regulated by the ubiquitination mediated by Keap1-Cul3 ubiquitin ligase complex and subsequent proteasomal degradation. ARE inducers impair the activity of the Keap1-Cul3 ubiquitin ligase, and the stabilized Nrf2 translocates into the nucleus, leading to transcriptional activation of ARE-driven protective genes.

(B) Domain structures of human Nrf2 and Keap1. Six conserved Neh1-6 domains are shown in colors, and DLG and ETGE motifs within Neh2 domain and putative ubiquitin acceptor lysines are indicated (hNrf2). Locations of all cysteines and important binding partners are shown, and three key cysteines (C151, C273, and C288) are highlighted in red (hKeap1).

LxxQDxDLG) and an ETGE motif (formulated as DxETGE), are recognized by a Keap1 homodimer, and the multiple lysine residues located between the two motifs are targeted for polyubiquitination by the Cul3-Keap1 E3 ligase complex.

In unstressed physiological conditions, Keap1 acts in the cytoplasm to down-regulate Nrf2's ability to activate transcription. Upon oxidative stress, Nrf2 escapes from Keap1-mediated repression and translocates to the nucleus, where it induces the transcription of ARE-directed genes (Figure 1A). Besides oxidative insult induced by radical species, small molecule electrophiles are also capable of inactivating Keap1 by modifying several cysteines (Dinkova-Kostova et al., 2002; Wakabayashi et al., 2004). Among 27 cysteines in human Keap1, three cysteines have been identified to be important modification sites for the suppression of Keap1. Cell-based mutational studies (Kobayashi et al., 2006; Zhang and Hannink, 2003) and in vivo studies (Yamamoto et al., 2008) have revealed that C273 and C288 in the IVR are required for Keap1-mediated ubiquitination of Nrf2, whereas C151 located in the BTB domain is required for Nrf2 to escape from Keap1 in response to ARE inducers. However, mass spectrometry analysis has detected a number of reactive cysteines that react with electrophiles (Hong et al., 2005; Luo et al., 2007), suggesting that more cysteine residues may contribute to modulating Keap1 activity. Here, we describe mass spectrometry and biochemical analysis of the **AI-1**–modified Keap1 and the study on its implication in the activity of Keap1 and Nrf2.

RESULTS

Discovery of a Small Molecule ARE Inducer, AI-1

In an effort to discover new ARE inducers that could be used as chemical tools to further explore the cellular biology and physiology of the ARE signaling pathways, we performed a high-throughput cell-based screen for compounds that are capable of activating the ARE in human neuroblastoma IMR-32 cells. For a screen of 1.2 million small molecules in 1,536-well format, the top hits (0.5%) were rescreened in triplicate under primary assay conditions and also in the presence of 1 mM of the antioxidant *N*-acetylcysteine to exclude hits arising from induction of oxidative stress. After a triage process that involved removal of compounds with undesirable functional groups and predicted nonspecific reactivity, the top 117 compounds were confirmed to the level of dose-response in the primary assay in 384-well plate format and were tested for the ARE and NQO1 activity in primary cortical culture (Johnson et al., 2002). After further prioritization, we identified seven final lead compounds that are available from commercial sources, all of which showed a single-digit micromolar potency in the reporter gene assays (Figure 2A). We chose the chloroquinolinone scaffold for further analysis, because this compound did not appear as electrophilic as some of the other compounds and exhibited low toxicity. We designated the compound as **AI-1** (ARE Inducer-1; Figure 2B) and demonstrated that it activates an ARE-dependent luciferase reporter with an EC_{50} of 2.7 ± 1.6 μM (n = 21) with 70%–80% efficacy compared to our positive control, *tert*-butylhydroquinone (tBHQ) (EC_{50}, 5–12 μM)

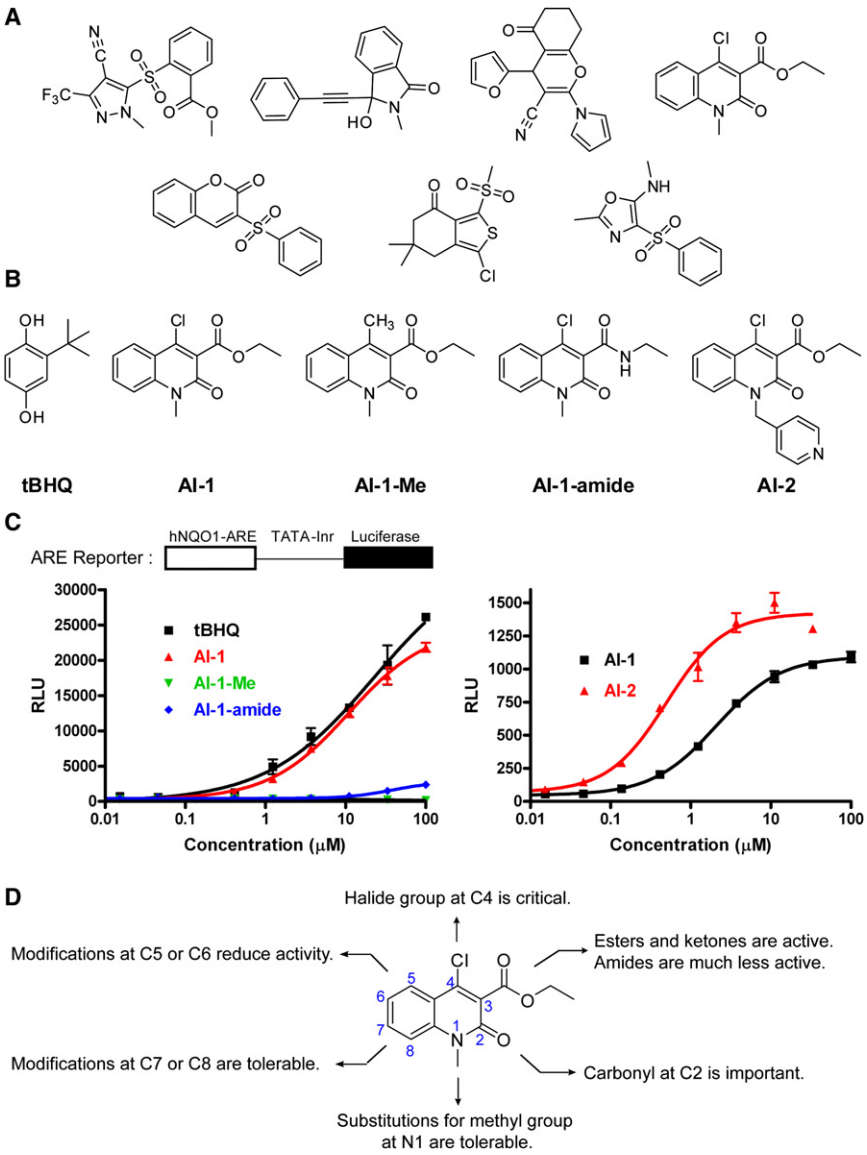

Figure 2. New Class Synthetic Nrf2/ARE Activator AI-1 and Its Analogs and Structure and Activity Relationship

(A) Structures of the seven lead ARE inducers identified from cellular screening of a 1.2 × 10^6 small-molecule library.

(B) Structures of tBHQ, **AI-1**, **AI-1-Me**, **AI-1-amide**, and **AI-2**.

(C) **AI-1** induces an hNQO1-ARE-coupled luciferase reporter in IMR-32 cells with a similar potency to tBHQ, whereas **AI-1-Me** and **AI-1-amide** show no and mild induction, respectively (left panel). **AI-2** shows roughly three times higher potency than **AI-1** in ARE-luc assay (right panel). Error bars indicate the standard deviations from triplicate samples.

(D) Summary of the SAR analysis.

(Figure 2C). **AI-1** failed to activate a mutant ARE where two nucleotides (GC) were substituted with AT within the core ARE sequence, even at a high concentration (30 μM) (see Figure S1 available online), demonstrating that this compound specifically triggered the ARE response.

Structure and Activity Relationship of AI-1

To investigate structure and activity relationship of **AI-1**, a variety of analogs were synthesized, and their activities were examined using ARE-luciferase reporter gene assay in IMR-32 cells. **AI-1** possesses an electrophilic aryl chloride group located at the β-position of two α,β-unsaturated carbonyl systems, which could potentially be displaced by nucleophilic thiols through a 1,4-addition-elimination reaction. To investigate the functional requirement of the aryl chloride group for the ability of compounds to induce the ARE response, we replaced the chloro substituent with a nonreactive methyl group (**AI-1-Me**) (Figure 2B). **AI-1-Me** lost all ability to activate the ARE up to a concentration of 100 μM (Figure 2C). We next prepared a number of analogs where the reactivity of the aryl chloride group was modulated by introducing electron donating or withdrawing functional groups (Figure 2D; Figure S2). Consistent with previous reports investigating ARE-inducing Michael acceptors (Dinkova-Kostova et al., 2001; Talalay et al., 1988), the SAR analysis of **AI-1** demonstrated that the electrophilicity of the reactive chloride determines the potency of the compounds. For example, the replacement of esters with ketones was tolerated, but replacement with amides or other less electron-withdrawing groups resulted in a significant reduction in the ARE-inducing activity. The amide analog of **AI-1**, **AI-1-amide** (Figure 2B) possessed 10% of the ARE-inducing activity of **AI-1** at a concentration of 100 μM (Figure 2C). Interestingly, an analog where the ester of **AI-1** was replaced with a strongly electron-withdrawing nitro group was only marginally active (compound **4b**) (Figure S2). This finding indicates that the reactivity of the halide group is not the sole determinant of activity and that other factors such as intracellular drug concentration and noncovalent recognition by intracellular target proteins may also be important. In addition, the SAR analysis also revealed that the carbonyl at C2 makes a significant contribution to the activity. Modifications of the sites that are located away from the reactive aryl chloride, such as the ethyl group of the ester and the methyl at N1, were tolerated. Similarly, modifications of C7 and C8 positions of the aromatic ring caused no major loss of activity, suggesting that these positions do not directly interact with the intracellular target protein. Through this analysis, we identified an active compound, **AI-2** (Figure 2B), that exhibited roughly three-fold more potent ARE-luc activity relative to **AI-1** (EC_{50}, 0.5–2.0 μM with 140% efficacy; Figure 2C). Because **AI-2** was identified later, most of the

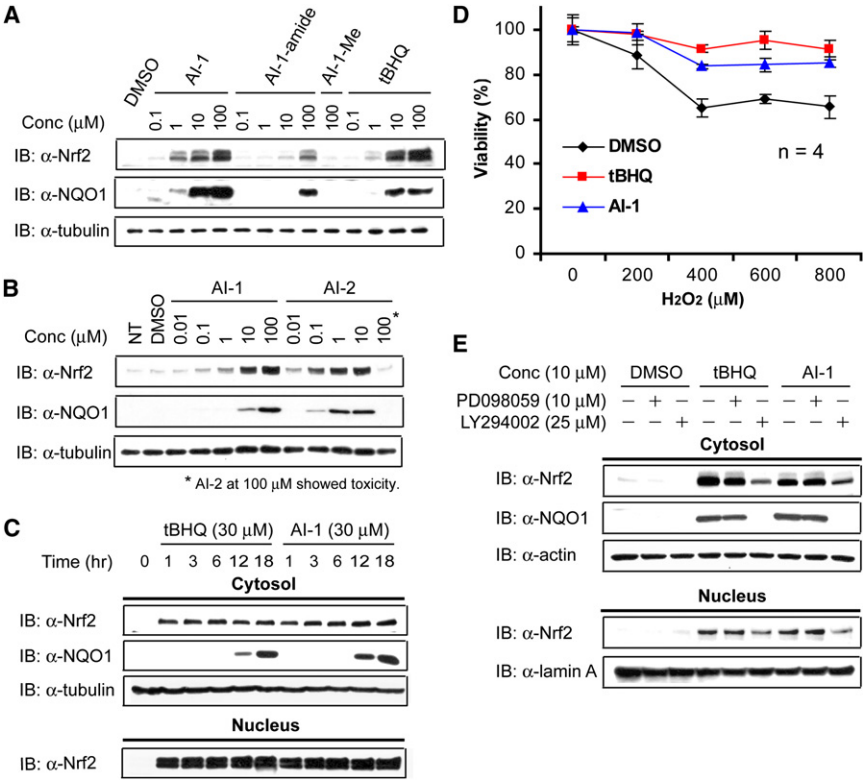

Figure 3. AI-1 Induces Stabilization/Nuclear Translocation of Nrf2 and Production of Downstream protective Genes

Panels show comparison of **AI-1** and its analogs with regard to their effects on the activity of Nrf2 and the expression of NQO1 in IMR-32 cells.

(A) Western blot analysis after 18 hr treatment showed that **AI-1** induces Nrf2 activation and NQO1 expression in a dose-dependent manner starting at 1 μM, whereas **AI-1-amide** has an effect only at 100 μM and **AI-1-Me** has no effect up to 100 μM.

(B) Dose-response analysis after 24 hr treatment indicated that **AI-2** is active at approximately 10-fold lower concentrations than **AI-1** with respect to Nrf2 activation and NQO1 expression.

(C) After treatment with 30 μM **AI-1**, Nrf2 stabilization/nuclear translocation initiated within 1 hr and reached a plateau after 3 hr. NQO1 expression appeared after 12 hr and continues to increase.

(D) IMR-32 cells pretreated with either tBHQ or **AI-1** (10 μM) for 48 hr became resistant to cell death induced by 1 hr treatment of H_2O_2. Error bars indicate the standard deviations from quadruplicate samples.

(E) Cotreatment with inhibitors of either MEK1 (PD098059, 10 μM) or PI3K (LY294002, 25 μM) for 24 hr followed by Western blot analysis of cytosolic and nuclear fractions revealed that PI3K activity is required for **AI-1** to both stabilize Nrf2 in cytosol and translocate Nrf2 into the nucleus.

mechanistic works have been focused on the original lead compound **AI-1**.

AI-1 Stabilizes Nrf2 and Induces Expression of Protective Enzymes

We investigated the ability of **AI-1**, **AI-1-Me**, **AI-1-amide**, and **AI-2** to stabilize Nrf2 and induce NQO1 expression in IMR-32 cells by measuring protein levels after treatment with various concentrations of the compounds for 18 hr (Figure 3A). **AI-1** was capable of inducing a dose-dependent increase of the levels of Nrf2 and NQO1, starting at a concentration of 1 μM, whereas **AI-1-amide** showed a substantial induction only at a concentration of 100 μM, and **AI-1-Me** showed no activation even at 100 μM. From a dose-response analysis after a 24 hr treatment, **AI-2** exhibited approximately 10-fold higher potency in Nrf2 activation and expression of NQO1 relative to **AI-1** (Figure 3B).

A time-course study with **AI-1** (30 μM) demonstrated that both stabilization and nuclear translocation of Nrf2 began within 1 hr and reached a plateau after 3 hr (Figure 3C). Expression of NQO1 was delayed and only appeared after 12 hr of treatment and then continued to increase. Notably, a slightly higher molecular weight band of Nrf2 was detected specifically in the nuclear fraction, which may correspond to phosphorylated Nrf2 localized in nucleus, as reported elsewhere (Apopa et al., 2008).

To investigate whether **AI-1** induces oxidative stress, which then might result in ARE activation, IMR-32 cells were pretreated with 1 mM *N*-acetylcysteine for 2 hr that prevented production of oxygen free radicals prior to treatment with **AI-1** for 24 hr (Figure S3). The levels of Nrf2 activation and NQO1 expression induced by tBHQ or **AI-1** (20 μM) were not reduced by pretreatment of 1 mM *N*-acetylcysteine, showing that oxidative stress is not involved in **AI-1**–mediated ARE activation in IMR-32 cells (Lee et al., 2001b).

To examine the cytoprotective effect of **AI-1**, IMR-32 cells were pretreated with 10 μM of either **AI-1** or tBHQ for 48 hr, followed by exposure to hydrogen peroxide (200−800 μM) for 1 hr, and viability was determined using an MTT assay ($n = 4$) (Figure 3D) (Li et al., 2002). **AI-1** and tBHQ exhibited similar protective effects against H_2O_2-induced apoptosis relative to the DMSO control. The degree of protection increased both with the time the cells were exposed to the ARE inducers and the concentration of H_2O_2. Although both tBHQ and **AI-1** protected cells against the acute toxicity generated by H_2O_2, unlike tBHQ, **AI-1** did not act as a free radical scavenger in vitro, as assessed by antioxidant capacity assays employing ABTS (2,2′-azino-bis(3-ethylbenzothiazoline-6-sulfonic acid) and DPPH (2,2-diphenyl-1-picrylhydrazyl) (Figure S4). These results are consistent with a model where the protective effect of **AI-1** against oxidative stress is mediated by Nrf2-mediated antioxidant response, not by radical scavenging properties.

AI-1-Mediated ARE Activation Is Dependent on PI3K Activity

The activities of several kinases, including MAPK, PI3K, PKC, CK2, and PERK, are implicated in the regulation of Nrf2 activity (Sherratt et al., 2004). It has been also shown that Nrf2 is a direct substrate of kinases such as PKC (Huang et al., 2002), CK2 (Apopa et al., 2008), and PERK (Cullinan et al., 2003) in vitro, suggesting that phosphorylation events may play an important role in regulating the activity of Nrf2. However, the kinases involved

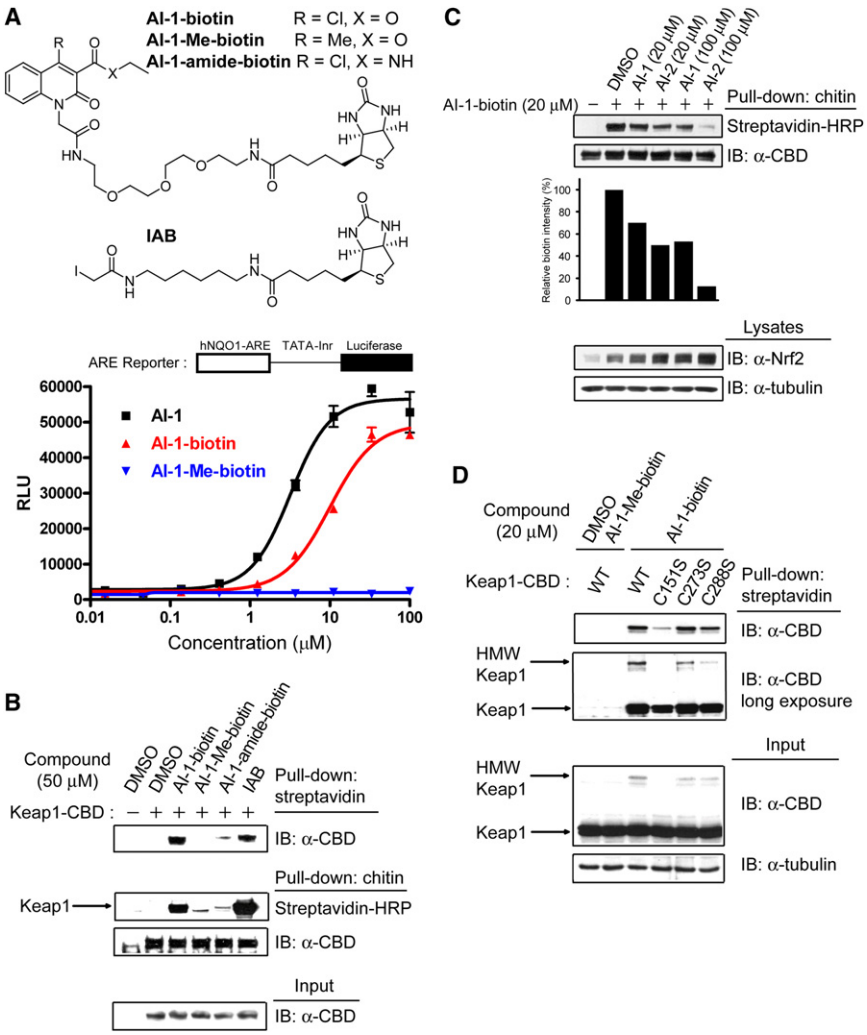

Figure 4. AI-1 Forms a Covalent Bond with Keap1 in Cells

(A) Chemical structures of **AI-1-biotin**, **AI-1-Me-biotin**, **AI-1-amide-biotin**, and **IAB** (upper panel). **AI-1-biotin** and **AI-1-Me-biotin** show similar activities relative to their parent compounds in ARE-luc assay using IMR-32 cells (lower panel). Error bars indicate the standard deviations from triplicate samples.

(B) Keap1-CBD transfected HEK293 cells were treated with the biotinylated compounds (50 μM) and biotin labeling of Keap1 was analyzed with streptavidin pull-down/CBD blot and chitin pull-down/streptavidin-HRP blot. The following order of reactivity toward Keap1 was determined: **AI-1-biotin** → **AI-1-amide-biotin** → **AI-1-Me-biotin**.

(C) **AI-1**, **AI-2** (20, 100 μM) were pretreated for 1 hr before treatment of **AI-1-biotin** (20 μM) for 3 hr. Chitin pull-down followed by streptavidin-HRP analysis indicated that **AI-2** alkylates Keap1 cysteines more vividly than **AI-1**. The band intensity was quantified using ImageJ software and biotin-labeled Keap1 was assessed by the intensity ratio of streptavidin/CBD relative to the ratio from the DMSO control.

(D) A similar labeling experiment with three different Keap1 cysteine mutants revealed that **AI-1-biotin** alkylates C151 primarily, and alkylates C273 and C288 to a lesser extent in cells.

in phosphorylation and activation of Nrf2 appear to be cell type dependent. It has been reported that ARE activation by tBHQ is dependent on the activity of PI3K, but not ERK, in IMR-32 cells (Lee et al., 2001a).To investigate whether the PI3K or MAPK pathway is required for **AI-1** to activate the ARE, IMR-32 cells were cotreated with **AI-1** and an inhibitor of either MEK1 (PD098059) or PI3K (LY294002) for 24 hr, and then cytosolic and nuclear fractions were analyzed. LY294002 (25 μM) but not PD098059 (10 μM) was capable of blocking Nrf2 stabilization and nuclear translocation and NQO1 expression induced by **AI-1** (10 μM) (Figure 3E). This finding suggests that PI3K activity is required for **AI-1** to both stabilize and translocate Nrf2 into nucleus.

AI-1 Irreversibly Labels Keap1 Primarily Through Reaction with Cys151 of Keap1

ARE-inducing activity has been detected from a variety of compounds, including natural products, compounds derived from a normal diet, synthetic drugs (Habeos et al., 2008), and metabolites (Surh, 1999). All reported small molecule ARE inducers contain thiol-reactive electrophilic centers that covalently modify the cysteine thiols of Keap1 and other thiol-containing proteins. In analogy to known ARE activators, we hypothesized that the chloro substituent of **AI-1** might react with one of the nucleophilic cysteines of Keap1. The reactive cysteines of Keap1 have been mapped using biotin-tagged electrophiles, such as iodoacetamide and *N*-alkylmaleimide, as labeling probes (Hong et al., 2005), but there are no reports of biotin-probes derivatized from well-characterized ARE inducers such as tBHQ (Gharavi et al., 2007) and sulforaphane (Juge et al., 2007). We therefore synthesized three biotinylated compounds where a linker was attached to the quinolinone nitrogen—a position we had previously demonstrated to tolerate a variety of functional groups without loss of ARE-inducing activity (**AI-1-biotin**, **AI-1-Me-biotin**, and **AI-1-amide-biotin**; Figure 4A). We used the ARE-luc reporter gene assay using IMR-32 cells to confirm that the biotinylated compounds were cell permeable and exhibited activity similar to that of their parent compounds. To investigate whether the biotinylated compounds could covalently modify Keap1, HEK293 cells were transfected with chitin-binding domain (CBD)–tagged wild-type (WT) Keap1 and treated with the biotinylated compounds at a concentration of 50 μM for 3 hr. As a positive control, a known Keap1-alkylating agent *N*-iodoacetyl-*N*-biotinylhexylenediamine (**IAB**, 50 μM; Figure 4A) was included (Hong et al., 2005). Pull-down with streptavidin beads and subsequent Western blot analysis using anti-CBD antibody showed high Keap1 alkylation by **AI-1-biotin**, modest alkylation

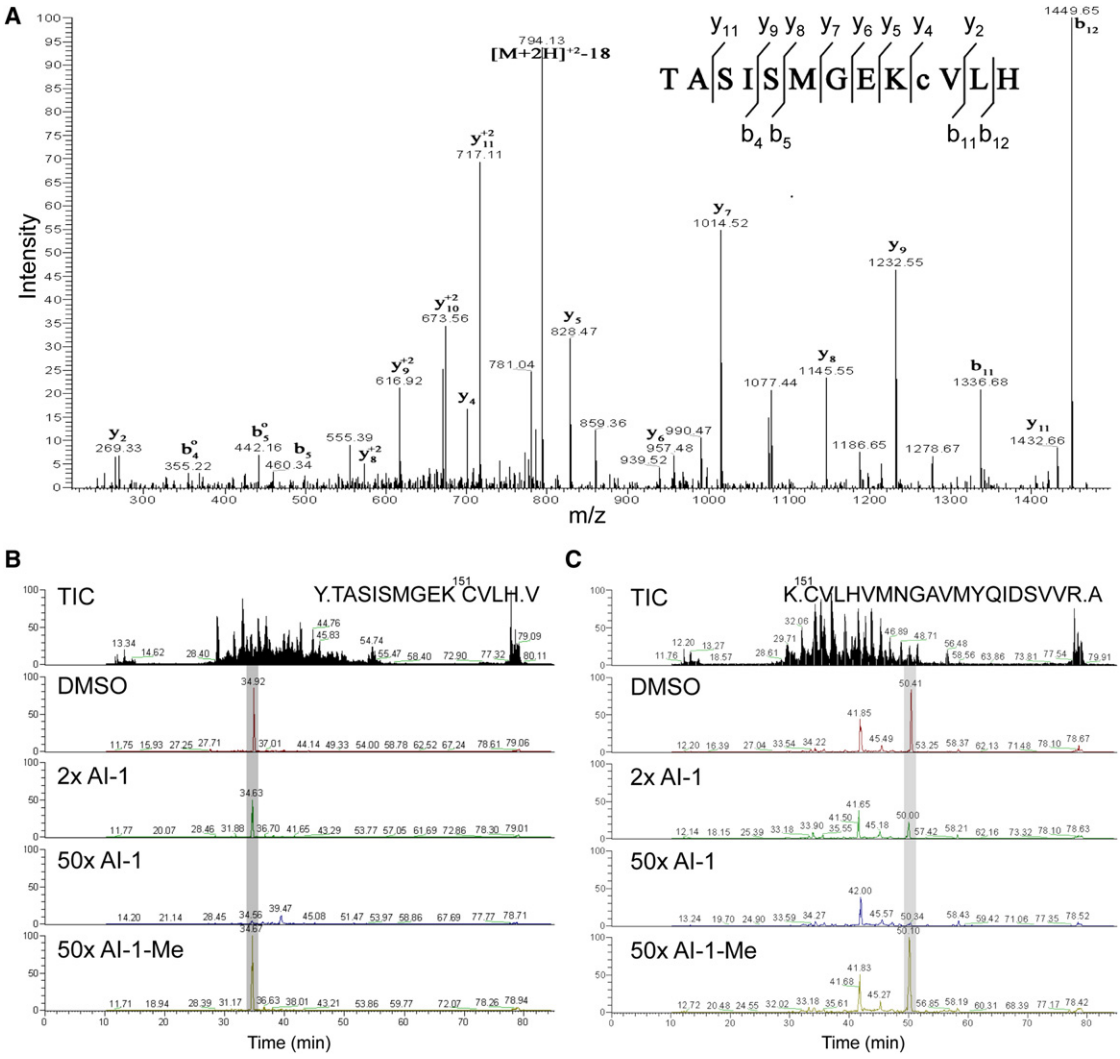

Figure 5. Cys151 of Keap1 Is Determined to Be the Major Site of Modification by AI-1 from Mass Spectrometry Analysis

(A) LC/MS/MS analysis of a chymotryptic digest (amino acid 142–154) following in vitro labeling of Keap1 with **AI-1** confirmed alkylation of Cys151 by **AI-1**.

(B and C) The signals of the unmodified (B) chymotryptic and (C) tryptic peptides that contain Cys151 measured on LTQ IonTrap were decreased by reaction with **AI-1**. The LC peaks for the peptides are highlighted in gray.

by **AI-1-amide-biotin**, and no alkylation by **AI-1-Me-biotin**. Similarly, pull-down with chitin beads followed by streptavidin-HRP blot analysis also showed the same order of alkylation levels: **AI-1-biotin** → **AI-1-amide-biotin** → **AI-1-Me-biotin** (Figure 4B).

AI-2 exhibited stronger ARE-inducing activity relative to **AI-1**, despite both compounds being predicted to possess electrophilic centers of comparable reactivity (Figures 2C and 3B). To investigate the molecular basis for this observation, we performed a comparative analysis of the reactivity of **AI-1** and **AI-2** toward Keap1 using **AI-1-biotin** as a means to quantify the extent of Keap1 labeling. HEK293 cells transfected with Keap1-CBD were treated with either **AI-1** or **AI-2** (20 and 100 μM, respectively) for 1 hr, followed by a washout and treatment with **AI-1-biotin** (20 μM) for another 3 hr. Chitin pull-down and subsequent analysis of biotinylated Keap1 revealed that **AI-2** masked Keap1 cysteines from being alkylated by **AI-1-biotin** to a greater extent than **AI-1** did (Figure 4C). This finding indicates that **AI-2** is more potent than **AI-1** in reacting with Keap1 and provides a potential explanation for its more potent ARE-inducing activity.

To identify which cysteines of Keap1 were alkylated, HEK293 cells were transfected with CBD-tagged Keap1 WT or mutants in which each of three preferred alkylating cysteines was replaced by serine (C151S, C273S, and C288S) and treated with 20 μM of the two biotin probes (**AI-1-biotin** or **AI-1-Me-biotin**) for 3 hr. Biotin-conjugated protein complexes were pulled down by streptavidin beads and subjected to immunoblot analysis with anti-CBD antibody. Interestingly, each mutant resulted in a different degree of alkylation. Alkylation was slightly reduced in the C273S mutant, more significantly reduced in the C288S mutant, and almost completely eliminated in the C151S mutant. The extent of labeling event was also proportional to the intensity of high-molecular-weight Keap1 (HMW Keap1) that was formed as a result

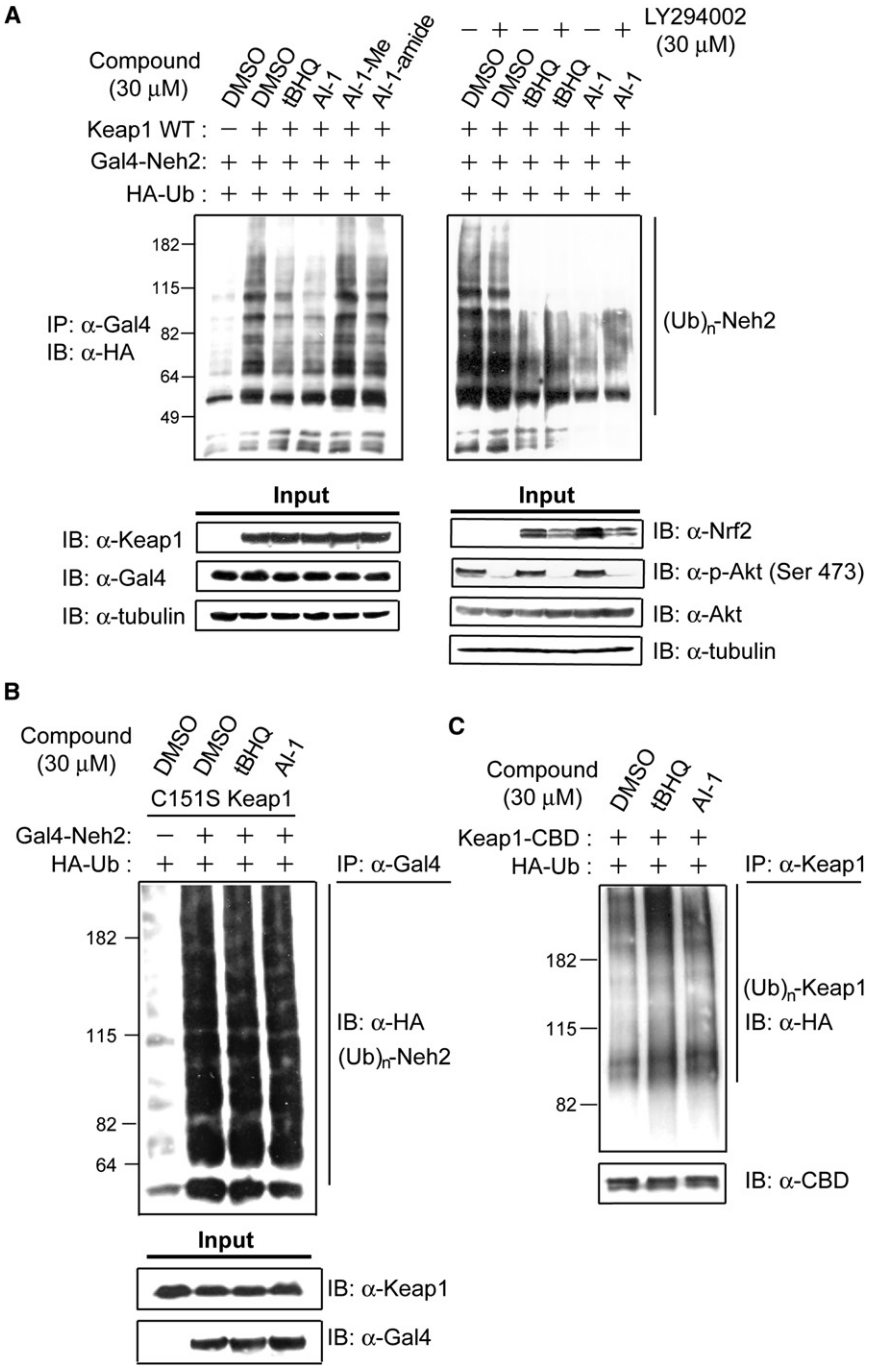

Figure 6. AI-1 Inhibits Keap1-Mediated Neh2 Ubiquitination In Vivo in a C151-Dependent Manner

(A and B) HEK293 cells were transiently transfected with Keap1, Gal4-Neh2, and HA-Ub and treated with tBHQ, **AI-1**, **AI-1-Me**, or **AI-1-amide** (30 μM) for 5 hr. Lysates were immunoprecipitated by anti-Gal4 antibody, and ubiquitination was assessed using anti-HA antibody.

(A) Both tBHQ and **AI-1** strongly inhibit Keap1-mediated Neh2 ubiquitination, whereas **AI-1-Me** and **AI-1-amide** show no and slight inhibition, respectively (left blot). Treatment with LY294002 (25 μM) does not reverse the inhibitory effect of tBHQ or **AI-1** on Neh2 ubiquitination (right blot).

(B) Neither tBHQ nor **AI-1** inhibits Neh2 ubiquitination in Keap1 C151S mutant-transfected cells.

(C) HEK293 cells were transiently transfected with Keap1-CBD and HA-Ub and treated with tBHQ, **AI-1** (50 μM) for 12 hr. Immunoprecipitation with anti-Keap1 antibody and immunoblot with anti-HA antibody revealed that **AI-1** induces Keap1 ubiquitination in vivo to a smaller extent relative to tBHQ.

of alkylation (Hong et al., 2005). The simplest explanation of these results is that alkylation of WT Keap1 by **AI-1** in cells occurs primarily on Cys151 in the BTB domain, with some alkylation on Cys288 and only minor alkylation on Cys273 in the IVR (Figure 4D).

We also conducted an unbiased analysis to discover more cysteine residues modified by **AI-1** in vitro. We expressed human Keap1 in *Escherichia coli* and incubated the recombinant Keap1 with **AI-1** (protein-to-compound molar ratio, 1:2) for MS analysis. Liquid chromatography coupled with tandem mass spectrometry (LC/MS/MS) analysis of the chymotryptic peptide covering Cys151 (amino acid 142–154) showed an increase of 229 in mass from all peptide fragments containing Cys151, indicating that Cys151 was alkylated by **AI-1** (Figure 5A). It was also confirmed by LC/MS results that the MS signals of the chymotryptic and tryptic peptide containing Cys151 were diminished by the reaction with **AI-1**, whereas no change was observed by the addition of **AI-1-Me** (Figures 5B and 5C). In addition to C151, covalent modifications at C23, C38, and C196 were also detected from LC/MS/MS analysis, albeit with less intensity (Table S1). Modification of these cysteines might also contribute to the inactivation of Keap1.

AI-1 Inhibits Keap1-Mediated Ubiquitination of Nrf2

We next determined whether treatment of cells with **AI-1** would inhibit Keap1-mediated Nrf2 ubiquitination. HEK293 cells were cotransfected with expression vectors for hemagglutinin-ubiquitin (HA-Ub), Gal4-fused Neh2 (amino acid 1–97 of Nrf2), and Keap1, and treated with 30 μM of each compound for 5 hr. Cell lysates were immunoprecipitated by anti-Gal4 antibody, and the immunopurified Neh2 domain was analyzed for the presence of ubiquitin by Western blot analysis using anti-HA antibody (Figure 6A). Both tBHQ and **AI-1** strongly inhibited Keap1-dependent Neh2 ubiquitination. **AI-1-amide** slightly inhibited the ubiquitination event, whereas **AI-1-Me** showed no inhibition. The inhibitory activity of each compound on Neh2 ubiquitination is well correlated with the effects on other molecular events associated

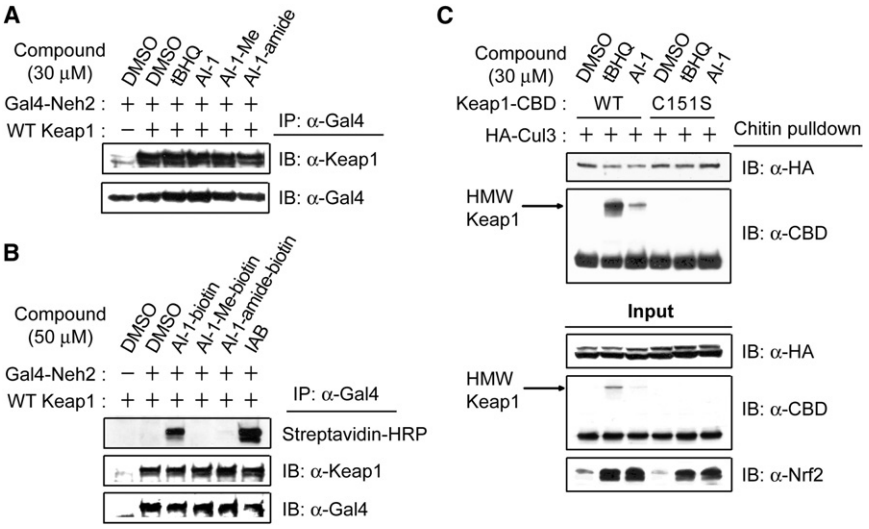

Figure 7. AI-1 Disrupts Keap1-Cul3 Interaction in a C151-Dependent Manner

(A and B) HEK293 cells were transiently transfected with Gal4-Neh2 and WT Keap1, and treated with compounds at (A) 30 μM or (B) 50 μM for 5 hr. The lysates were immunoprecipitated using an anti-Gal4 antibody, and the level of copurified Keap1 was measured.

(A) Copurification of Keap1 was not affected by treatment with the compounds that possessed different electrophilicity.

(B) Treatment with biotin probes did not change the binding affinity between Keap1 and Neh2 domain, although the copurified Keap1 was labeled with biotin to a different extent.

(C) HEK293 cells were transiently transfected with HA-Cul3 and CBD-tagged WT (or C151S) Keap1, and treated with tBHQ or **AI-1** (30 μM) for 5 hr. Pull-down using chitin beads and ensuing immunoblot analysis with anti-HA antibody showed that both tBHQ and **AI-1** destabilize the interaction between Keap1 and Cul3 in HEK293 cells in a C151-dependent manner.

with the ARE activation, including Nrf2 stabilization and nuclear translocation, Keap1 alkylation, and ARE-luc induction. Neither tBHQ nor **AI-1** was able to protect Nrf2 from ubiquitination in cells expressing the C151S-Keap1 mutant (Figure 6B), indicating that **AI-1** inhibits Keap1-driven ubiquitination of Nrf2 in a C151-dependent manner.

We then investigated how the PI3K pathway is involved in regulation of Nrf2. We performed the in vivo Neh2 ubiquitination assay following treatment of 30 μM of ARE inducers and 25 μM of LY294002 for 5 hr (Figure 6A). Interestingly, the PI3K inhibitor did not override the inhibitory effect of tBHQ or **AI-1** on Neh2 ubiquitination, although it did down-regulate the endogenous Nrf2 activated by either ARE inducer. In addition, this PI3K-independent regime was also observed for the ubiquitination of both endogenous and overexpressed full-length Nrf2 in HEK293 cells (Figures S5A and S5B). These results suggest that phosphorylation of Nrf2 by kinases located downstream of PI3K may be involved in the regulation after Nrf2 is relieved from Keap1-mediated down-regulation. We next investigated whether the PI3K pathway might modulate Nrf2 at the translation level. We examined the synthesis of endogenous Nrf2 using a ^{35}S-labeling assay. HEK293 cells were treated with **AI-1** (30 μM) together with LY294002 (20 μM) for 4 hr and were exposed to ^{35}S-methionine/^{35}S-cysteine containing media for 45 min (Figure S5C). Immunoprecipitation and analysis of ^{35}S-labeled Nrf2 demonstrated that treatment of LY294002 down-regulates the translation of basal and induced Nrf2. Together these results indicate that PI3K signaling modulates Nrf2 at the level of protein translation rather than protein stability.

Keap1-alkylating ARE inducers, such as tBHQ and sulforaphane, elicit autoubiquitination of Keap1, although its biological implication is unclear. It has been proposed that alkylation of Keap1 by electrophiles switches the ubiquitination target from Nrf2 to Keap1 (Hong et al., 2005; Zhang et al., 2005). To see whether **AI-1** also causes Keap1 ubiquitination, Keap1 ubiquitination was examined following treatment of either tBHQ or **AI-1** (50 μM) for 12 hr to HEK293 cells that were transiently transfected with Keap1 and HA-Ub (Figure 6C). Interestingly, although tBHQ and **AI-1** showed a similar potency in inhibition of Keap1-mediated Nrf2 ubiquitination, **AI-1** induced Keap1 autoubiquitination to a smaller extent than tBHQ. which suggests that tBHQ and **AI-1** interact with Keap1 cysteines in different modes to repress the function of Keap1.

AI-1 Inhibits Nrf2 Ubiquitination by Disrupting the Interaction Between Cul3 and Keap1

We next investigated the ability of **AI-1** to influence the association of Keap1 with Nrf2. HEK293 cells were transfected with expression vectors for Gal4-Neh2 and WT Keap1 and treated with **AI-1** and its analogs (30 μM) for 5 hr. The level of copurified Keap1 was analyzed by Western blot analysis following immunoprecipitation with anti-Gal4 antibody (Figure 7A). The level of copurified Keap1 was not changed by treatment of either compound. In a second experiment, the cotransfected HEK293 cells were treated with biotinylated compounds (**AI-1-biotin**, **AI-1-Me-biotin**, and **AI-1-amide-biotin**, 50 μM) for 5 hr, and cell lysates were immunoprecipitated with anti-Gal4 antibody (Figure 7B). Western blot analysis with anti-Keap1 antibody showed that Keap1 copurification was not affected by the treatment with the biotinylated compounds, although the copurified Keap1 was biotin-labeled to a different extent, as shown by streptavidin-HRP blot analysis. Together, these results suggest that alkylation by **AI-1** did not cause dissociation of the Nrf2-Keap1 complex.

Evidence demonstrated that alkylation of Keap1 by electrophiles promotes the dissociation of the Keap1-Cul3 interaction, leading to Nrf2 stabilization (Gao et al., 2007; Kobayashi et al., 2006; Zhang et al., 2004). To investigate whether this is also observed for **AI-1**, HEK293 cells were cotransfected with plasmids encoding HA-Cul3 and Keap1-CBD and were exposed to tBHQ and **AI-1** (30 μM) for 5 hr. Pull-down with chitin beads followed by immunoblot with anti-HA antibody revealed that both **AI-1** and tBHQ caused dissociation of the Keap1-Cul3 interaction (Figure 7C). The disruption of the Keap1-Cul3 interaction was not observed when the C151S Keap1 mutant was used instead. This result demonstrates that the alkylation of Keap1 C151 by **AI-1** is required for dissociation of the Keap1-Cul3

complex, which is a critical event for stabilization of Nrf2 and activation of the ARE pathway. Although both tBHQ and **AI-1** generated HMW Keap1 as a result of covalent reaction, **AI-1** produced HMW Keap1 to a much smaller extent than a phenolic antioxidant tBHQ. The similar potency of tBHQ and **AI-1** to impair the Keap1-Cul3 interaction indicates that the formation of the HMW Keap1 does not cause the Keap1-Cul3 dissociation.

We also compared **AI-1** and **AI-2** with respect to their ability to disrupt the Keap1-Cul3 interaction (Figure S6). Dose-response analysis revealed that **AI-2** is slightly more potent to disrupt the Keap1-Cul3 interaction than **AI-1**. These studies suggest a model whereby the stronger Nrf2/ARE-inducing activity of **AI-2** (Figures 2C and 3B) can be explained by more rapid Keap1 alkylation (Figure 4C), which causes more efficient dissociation of Keap1 from Cul3 (Figure S6). Further investigation will be required to determine whether **AI-2** is simply accumulated in cells to a greater extent than **AI-1** or whether it possesses superior noncovalent interaction with Keap1 that predisposes it to more efficient covalent bond formation.

AI-1 Reacts with a Number of Intracellular Proteins

We attempted to identify other intracellular targets of **AI-1** using the **AI-1-biotin** probe in conjunction with mass spectrometry. **AI-1-biotin** and **AI-1-Me-biotin** (50 μM) were treated to HEK293 cells, and biotin-labeled proteins were pulled down using streptavidin beads (Figure S7A). The specific band at 65 kDa from **AI-1-biotin** and the equivalent bands from DMSO and **AI-1-Me-biotin** that served as negative controls were subjected to LC/MS/MS analysis. The list of **AI-1**-specific binding proteins was obtained after the proteins detected from either negative control were subtracted (Figure S7B and Table S2). Among the **AI-1**-specific proteins, reactive cysteine-containing enzymes such as phosphatase (PP2A) and cysteine-rich ubiquitin E3 ligase (ARIH1) were identified, illustrating the ability of **AI-1** to target cysteines in various classes of proteins. Interestingly, histone deacetylase1/2 (HDAC1/2) was identified as binding proteins. In analogy to the proposed mechanism of HDAC inhibition by an ARE inducer sulforaphane (Myzak et al., 2004, 2006), a metabolic product of **AI-1**, as a result of its covalent reaction with intracellular cysteine, may also be able to inhibit HDAC1/2 and evoke the related biological effects. A subset of the identified proteins could be related to Nrf2/ARE pathway, but we think that Keap1-alkylation is sufficient to account for the ARE-inducing activity of **AI-1** because of the ability of the Keap1 C151S mutant to induce resistance to the compound. In-depth molecular analysis about whether any of these additional targets are involved in Keap1/Nrf2 regulation is currently under investigation.

DISCUSSION

The activation of the Nrf2-ARE pathway is initiated by covalent modifications of cysteine thiols of Keap1 by electrophiles, radicals, or heavy metals. Although all of these species are destined to enhance transcriptional activity of Nrf2, the detailed mechanisms by which these species suppress the activity of Keap1 are not the same. For example, studies have shown that Keap1 modification by electrophiles, such as tBHQ and sulforaphane, dissociates the Keap1-Cul3 interaction in a C151-dependent manner, whereas some heavy metals, such as arsenic species, promote the association of the two proteins in a C151-independent fashion (Wang et al., 2008). There might be more mechanisms yet for sensing thiol-reacting agents and perturbing Keap1 activity that are required for Nrf2-driven antioxidant response.

In this paper, we reported the discovery and characterization of a new class of small-molecule ARE inducer, **AI-1**. **AI-1** bears a reactive chloride that is located at the 4-position of two α,β-unsaturated carbonyl systems and that undergoes a nucleophilic aromatic substitution reaction with Keap1 cysteines. **AI-1** activates the Nrf2-ARE pathway, induces expression of antioxidant proteins such as NQO1, and increases cell survival in the condition of H_2O_2-induced oxidative stress. Functional analysis of **AI-1** and related analogs that exhibit a broad range of the electrophilicity revealed that the key target protein of **AI-1** is Keap1 and that the electrophilicity of the compound is necessary for its activity. As seen with tBHQ and sulforaphane, the formation of a covalent bond with Cys151 of Keap1 was the most important event underlying **AI-1**–driven Nrf2-ARE activation.

A unique and advantageous characteristic of **AI-1**, rarely seen from other ARE inducers, is the ease with which ARE-inducing activity can be modulated by altering electrophilicity or noncovalent recognition features of the scaffold. As a result, we were able to interrogate the extensive SAR analysis and obtain more potent analogs such as **AI-2**. The discovery of **AI-2**, whose electrophilicity should be similar to that of **AI-1**, suggests that noncovalent recognition of the small molecule by Keap1 may also be a significant contributor to the potency and efficacy of ARE-inducing small molecules. The SAR also revealed that the size of the substitutent at the C4 position was crucial for recognition by Keap1. For example, the chloride of **AI-1** could be replaced by a bromide but not by a larger tosyl group (compound **1d**) (Figure S2).

The SAR analysis enabled us to derivatize **AI-1** with a linker without losing ARE-inducing activity, leading to the synthesis of a nontoxic, cell-permeable biotinylated compound, **AI-1-biotin**. It served as a valuable probe to investigate the consequences of alkylating Keap1. We exploited **AI-1-biotin** to assess the relative reactivity of three important Keap1 cysteines (C151, C273, and C288) in cells and determined that C151 is the most reactive nucleophile toward **AI-1**. Further study will be required to investigate how reaction with the reactive C151 regulates Keap1 activity. It has been proposed that C151 alkylation might induce a conformational change of Keap1 to expose the two additional cysteines, C273 and C288, located in the IVR for alkylation (Zhang and Hannink, 2003). It may be also possible that cooperative modifications at C151 and C273/C288 by **AI-1** might lead to the inhibition of Keap1-mediated Nrf2 ubiquitination.

The detailed SAR of **AI-1** shown in this article may provide insight for designing ARE inducers. As demonstrated by **AI-2**, further medicinal chemistry efforts on **AI-1** or other lead compounds could lead to discovery of more powerful ARE inducers. **AI-1** and analogs may also find utility in exploring the therapeutic benefits of ARE activators in animal models of conditions where oxidative stress is implicated (Klaunig and Kamendulis, 2004).

SIGNIFICANCE

The Keap1-Nrf2-antioxidant response element (ARE) pathway is the major signaling pathway for sensing oxidative and environmental stress and for inducing a protective cellular response. Several electrophilic small molecules that stimulate this pathway have been reported to possess therapeutic benefit under stress-related conditions, such as neurodegeneration and carcinogenesis, owing to their ability to induce the expression of a wide range of protective proteins. Besides the utility in therapeutics, small-molecule ARE inducers can be pharmacological tools of the cellular antioxidant response. Here, we reported the discovery of a novel quinolinone-based ARE inducer (AI-1) that was identified from unbiased high-throughput screening of a small-molecule library. AI-1 is the first ARE inducer that is sensed by the cysteines of intracellular redox sensor Keap1 through a nucleophilic aromatic substitution reaction. On the basis of the effects on Keap1, such as formation of a high-molecular-weight Keap1 and autoubiquitination, AI-1 is functionally similar to sulforaphane rather than tBHQ. However, unlike sulforaphane, the chemical, structural feature of AI-1 allows the generation of a wide range of functional analogs. The SAR analysis revealed that both the reactivity of the electrophilic site and the noncovalent recognition features of the compound control the potency of the compound. Our study revealed that Cys151 is the most reactive residue toward AI-1 among the 27 cysteines of human Keap1 and that covalent modification of Cys151 disrupted the ability of Keap1 to serve as an adaptor for Cul3-ubiquitin E3 ligase complex, thereby leading to AI-1-driven Nrf2 activation. The mechanism of the Nrf2/ARE activation and the mode of interaction with Keap1, as demonstrated with AI-1, are likely to be applicable to other classes of cysteine-reactive small molecules.

EXPERIMENTAL PROCEDURES

ARE-Luciferase Reporter Gene Assay

hNQO1-ARE-luc reporter gene constructs (Moehlenkamp and Johnson, 1999) used for cell-based reporter gene assay were provided by Dr. Jeffrey Johnson (University of Wisconsin, Madison), and the sequence information of both WT and mutant ARE-luc is described in literature (Lee et al., 2001b) and in Figure S1. ARE-luc construct (100 ng/well) was transiently transfected to IMR-32 cells (10,000 cells, 60 μL/well) in white 384-well plates (Corning) using Fugene6 (Roche) following the manufacturer's procedure. After 24 hr transfection, preplated compounds that were prediluted into dose-response format (three-fold dilution, 12 points) ranging from 10 mM were transferred (600 nL) to the assay plates using a 384-pin transfer device. Each concentration was tested in triplicate. After 24 hr incubation in a cell incubator, BrightGlo (30 μL, Promega) was added and luminescence was quantified by using Envision multilabel plate reader (PerkinElmer). EC_{50} values were calculated using GraphPad Prism 4 (GraphPad Software). For the test of compounds in the presence of 1 mM *N*-acetylcysteine, cells (50 μL/well) were transfected for 24 hr and treated with 10 μl of 6 mM *N*-acetylcysteine in cell media (pH 7.4) for 2 hr prior to compound addition.

In Vivo Ubiquitination Assay

In vivo ubiquitination assay was performed as reported elsewhere (Buschmann et al., 2000) with a minor modification. HEK293 cells in a six-well plate were transfected with cDNAs encoding Keap1, Gal4-tagged Neh2 (or HA-tagged Nrf2), and HA-tagged ubiquitin. After washing with cold PBS, cells were lysed with 2% SDS in TBS (10 mM Tris-HCl [pH 8.0] and 150 mM NaCl) at 95°C for 10 min and were sonicated for 20 s at 4°C. Eight volumes of 1% Triton X-100 in TBS were added, and the solution was incubated for 30 min at 4°C with Protein G beads (Roche) and clarified by 1 min centrifugation (20,000 *g*) at 4°C. The protein solution (supernatant) was incubated with anti-Gal4 antibody (Santa Cruz Biotechnology) for 1 hr at 4°C before overnight incubation with Protein G beads at 4°C. The beads were washed with 0.5 M LiCl in TBS followed by two additional washes with TBS. Proteins were loaded onto 8% SDS-PAGE gel, and subjected to immunoblot analysis with anti-HA antibody (Covance).

For in vivo ubiquitination of endogenous Nrf2, HEK293 cells were seeded in 100-mm dishes and treated with 10 μM MG132, 30 μM LY294002, 30 μM tBHQ, and 30 μM **AI-1** for 4 hr. Cells were lysed with TBS buffer containing 2% SDS, boiled, and sonicated. The resulting lysates were diluted 5 times with TBS buffer and were then subjected to immunoprecipitation with anti-Nrf2 antibody (C20, Santa Cruz Biotechnology) and immunoblot with anti-ubiquitin antibody (σ).

SUPPLEMENTAL INFORMATION

Supplemental information contains seven figures, two tables, and Supplemental Experimental Procedures and can be found with this article online at doi:10.1016/j.chembiol.2010.03.013.

ACKNOWLEDGMENTS

This work was supported by the Ellison Medical Foundation (P.G.S.), the American Heart Association (H.L.), and the Evelyn F. and William L. McKnight Brain Institute of the University of Florida (H.L.). We thank Jonathan Kern for assistance with the screens. The authors declare no competing financial interests.

Received: April 10, 2009
Revised: March 18, 2010
Accepted: March 26, 2010
Published: May 27, 2010

REFERENCES

Apopa, P.L., He, X., and Ma, Q. (2008). Phosphorylation of Nrf2 in the transcription activation domain by casein kinase 2 (CK2) is critical for the nuclear translocation and transcription activation function of Nrf2 in IMR-32 neuroblastoma cells. J. Biochem. Mol. Toxicol. *22*, 63–76.

Buschmann, T., Fuchs, S.Y., Lee, C.G., Pan, Z.Q., and Ronai, Z. (2000). SUMO-1 modification of Mdm2 prevents its self-ubiquitination and increases Mdm2 ability to ubiquitinate p53. Cell *101*, 753–762.

Cullinan, S.B., Zhang, D., Hannink, M., Arvisais, E., Kaufman, R.J., and Diehl, J.A. (2003). Nrf2 is a direct PERK substrate and effector of PERK-dependent cell survival. Mol. Cell. Biol. *23*, 7198–7209.

Dinkova-Kostova, A.T., Massiah, M.A., Bozak, R.E., Hicks, R.J., and Talalay, P. (2001). Potency of Michael reaction acceptors as inducers of enzymes that protect against carcinogenesis depends on their reactivity with sulfhydryl groups. Proc. Natl. Acad. Sci. USA *98*, 3404–3409.

Dinkova-Kostova, A.T., Holtzclaw, W.D., Cole, R.N., Itoh, K., Wakabayashi, N., Katoh, Y., Yamamoto, M., and Talalay, P. (2002). Direct evidence that sulfhydryl groups of Keap1 are the sensors regulating induction of phase 2 enzymes that protect against carcinogens and oxidants. Proc. Natl. Acad. Sci. USA *99*, 11908–11913.

Dinkova-Kostova, A.T., Holtzclaw, W.D., and Kensler, T.W. (2005). The role of Keap1 in cellular protective responses. Chem. Res. Toxicol. *18*, 1779–1791.

Furukawa, M., and Xiong, Y. (2005). BTB protein Keap1 targets antioxidant transcription factor Nrf2 for ubiquitination by the Cullin 3-Roc1 ligase. Mol. Cell. Biol. *25*, 162–171.

Gao, L., Wang, J., Sekhar, K.R., Yin, H., Yared, N.F., Schneider, S.N., Sasi, S., Dalton, T.P., Anderson, M.E., Chan, J.Y., et al. (2007). Novel n-3 fatty acid

oxidation products activate Nrf2 by destabilizing the association between Keap1 and Cullin3. J. Biol. Chem. *282*, 2529–2537.

Gharavi, N., Haggarty, S., and El-Kadi, A.O. (2007). Chemoprotective and carcinogenic effects of tert-butylhydroquinone and its metabolites. Curr. Drug Metab. *8*, 1–7.

Habeos, I.G., Ziros, P.G., Chartoumpekis, D., Psyrogiannis, A., Kyriazopoulou, V., and Papavassiliou, A.G. (2008). Simvastatin activates Keap1/Nrf2 signaling in rat liver. J. Mol. Med. *86*, 1279–1285.

Halliwell, B. (2007). Biochemistry of oxidative stress. Biochem. Soc. Trans. *35*, 1147–1150.

Hong, F., Sekhar, K.R., Freeman, M.L., and Liebler, D.C. (2005). Specific patterns of electrophile adduction trigger Keap1 ubiquitination and Nrf2 activation. J. Biol. Chem. *280*, 31768–31775.

Huang, H.C., Nguyen, T., and Pickett, C.B. (2002). Phosphorylation of Nrf2 at Ser-40 by protein kinase C regulates antioxidant response element-mediated transcription. J. Biol. Chem. *277*, 42769–42774.

Itoh, K., Wakabayashi, N., Katoh, Y., Ishii, T., Igarashi, K., Engel, J.D., and Yamamoto, M. (1999). Keap1 represses nuclear activation of antioxidant responsive elements by Nrf2 through binding to the amino-terminal Neh2 domain. Genes Dev. *13*, 76–86.

Johnson, D.A., Andrews, G.K., Xu, W., and Johnson, J.A. (2002). Activation of the antioxidant response element in primary cortical neuronal cultures derived from transgenic reporter mice. J. Neurochem. *81*, 1233–1241.

Juge, N., Mithen, R.F., and Traka, M. (2007). Molecular basis for chemoprevention by sulforaphane: a comprehensive review. Cell. Mol. Life Sci. *64*, 1105–1127.

Katoh, Y., Itoh, K., Yoshida, E., Miyagishi, M., Fukamizu, A., and Yamamoto, M. (2001). Two domains of Nrf2 cooperatively bind CBP, a CREB binding protein, and synergistically activate transcription. Genes Cells *6*, 857–868.

Kensler, T.W., Wakabayashi, N., and Biswal, S. (2007). Cell survival responses to environmental stresses via the Keap1-Nrf2-ARE pathway. Annu. Rev. Pharmacol. Toxicol. *47*, 89–116.

Klaunig, J.E., and Kamendulis, L.M. (2004). The role of oxidative stress in carcinogenesis. Annu. Rev. Pharmacol. Toxicol. *44*, 239–267.

Kobayashi, M., and Yamamoto, M. (2006). Nrf2-Keap1 regulation of cellular defense mechanisms against electrophiles and reactive oxygen species. Adv. Enzyme Regul. *46*, 113–140.

Kobayashi, A., Kang, M.I., Okawa, H., Ohtsuji, M., Zenke, Y., Chiba, T., Igarashi, K., and Yamamoto, M. (2004). Oxidative stress sensor Keap1 functions as an adaptor for Cul3-based E3 ligase to regulate proteasomal degradation of Nrf2. Mol. Cell. Biol. *24*, 7130–7139.

Kobayashi, A., Kang, M.I., Watai, Y., Tong, K.I., Shibata, T., Uchida, K., and Yamamoto, M. (2006). Oxidative and electrophilic stresses activate Nrf2 through inhibition of ubiquitination activity of Keap1. Mol. Cell. Biol. *26*, 221–229.

Lee, J.M., Hanson, J.M., Chu, W.A., and Johnson, J.A. (2001a). Phosphatidylinositol 3-kinase, not extracellular signal-regulated kinase, regulates activation of the antioxidant-responsive element in IMR-32 human neuroblastoma cells. J. Biol. Chem. *276*, 20011–20016.

Lee, J.M., Moehlenkamp, J.D., Hanson, J.M., and Johnson, J.A. (2001b). Nrf2-dependent activation of the antioxidant responsive element by tert-butylhydroquinone is independent of oxidative stress in IMR-32 human neuroblastoma cells. Biochem. Biophys. Res. Commun. *280*, 286–292.

Li, J., Lee, J.M., and Johnson, J.A. (2002). Microarray analysis reveals an antioxidant responsive element-driven gene set involved in conferring protection from an oxidative stress-induced apoptosis in IMR-32 cells. J. Biol. Chem. *277*, 388–394.

Luo, Y., Eggler, A.L., Liu, D., Liu, G., Mesecar, A.D., and van Breemen, R.B. (2007). Sites of alkylation of human keap1 by natural chemoprevention agents. J. Am. Soc. Mass Spectrom. *18*, 2226–2232.

Moehlenkamp, J.D., and Johnson, J.A. (1999). Activation of antioxidant/electrophile-responsive elements in IMR-32 human neuroblastoma cells. Arch. Biochem. Biophys. *363*, 98–106.

Myzak, M.C., Karplus, P.A., Chung, F.L., and Dashwood, R.H. (2004). A novel mechanism of chemoprotection by sulforaphane: inhibition of histone deacetylase. Cancer Res. *64*, 5767–5774.

Myzak, M.C., Dashwood, W.M., Orner, G.A., Ho, E., and Dashwood, R.H. (2006). Sulforaphane inhibits histone deacetylase in vivo and suppresses tumorigenesis in Apc-minus mice. FASEB J. *20*, 506–508.

Padmanabhan, B., Tong, K.I., Ohta, T., Nakamura, Y., Scharlock, M., Ohtsuji, M., Kang, M.I., Kobayashi, A., Yokoyama, S., and Yamamoto, M. (2006). Structural basis for defects of Keap1 activity provoked by its point mutations in lung cancer. Mol. Cell *21*, 689–700.

Sherratt, P.J., Huang, H.C., Nguyen, T., and Pickett, C.B. (2004). Role of protein phosphorylation in the regulation of NF-E2-related factor 2 activity. Methods Enzymol. *378*, 286–301.

Surh, Y. (1999). Molecular mechanisms of chemopreventive effects of selected dietary and medicinal phenolic substances. Mutat. Res. *428*, 305–327.

Surh, Y.J. (2003). Cancer chemoprevention with dietary phytochemicals. Nat. Rev. Cancer *3*, 768–780.

Talalay, P., De Long, M.J., and Prochaska, H.J. (1988). Identification of a common chemical signal regulating the induction of enzymes that protect against chemical carcinogenesis. Proc. Natl. Acad. Sci. USA *85*, 8261–8265.

Tong, K.I., Katoh, Y., Kusunoki, H., Itoh, K., Tanaka, T., and Yamamoto, M. (2006). Keap1 recruits Neh2 through binding to ETGE and DLG motifs: characterization of the two-site molecular recognition model. Mol. Cell. Biol. *26*, 2887–2900.

van Muiswinkel, F.L., and Kuiperij, H.B. (2005). The Nrf2-ARE signalling pathway: promising drug target to combat oxidative stress in neurodegenerative disorders. Curr. Drug Targets *4*, 267–281.

Wakabayashi, N., Dinkova-Kostova, A.T., Holtzclaw, W.D., Kang, M.I., Kobayashi, A., Yamamoto, M., Kensler, T.W., and Talalay, P. (2004). Protection against electrophile and oxidant stress by induction of the phase 2 response: fate of cysteines of the Keap1 sensor modified by inducers. Proc. Natl. Acad. Sci. USA *101*, 2040–2045.

Wang, X., Tomso, D.J., Chorley, B.N., Cho, H.Y., Cheung, V.G., Kleeberger, S.R., and Bell, D.A. (2007). Identification of polymorphic antioxidant response elements in the human genome. Hum. Mol. Genet. *16*, 1188–1200.

Wang, X.J., Sun, Z., Chen, W., Li, Y., Villeneuve, N.F., and Zhang, D.D. (2008). Activation of Nrf2 by arsenite and monomethylarsonous acid is independent of Keap1-C151: enhanced Keap1-Cul3 interaction. Toxicol. Appl. Pharmacol. *230*, 383–389.

Wasserman, W.W., and Fahl, W.E. (1997). Functional antioxidant responsive elements. Proc. Natl. Acad. Sci. USA *94*, 5361–5366.

Yamamoto, T., Suzuki, T., Kobayashi, A., Wakabayashi, J., Maher, J., Motohashi, H., and Yamamoto, M. (2008). Physiological significance of reactive cysteine residues of Keap1 in determining Nrf2 activity. Mol. Cell. Biol. *28*, 2758–2770.

Zhang, D.D. (2006). Mechanistic studies of the Nrf2-Keap1 signaling pathway. Drug Metab. Rev. *38*, 769–789.

Zhang, D.D., and Hannink, M. (2003). Distinct cysteine residues in Keap1 are required for Keap1-dependent ubiquitination of Nrf2 and for stabilization of Nrf2 by chemopreventive agents and oxidative stress. Mol. Cell. Biol. *23*, 8137–8151.

Zhang, D.D., Lo, S.C., Cross, J.V., Templeton, D.J., and Hannink, M. (2004). Keap1 is a redox-regulated substrate adaptor protein for a Cul3-dependent ubiquitin ligase complex. Mol. Cell. Biol. *24*, 10941–10953.

Zhang, D.D., Lo, S.C., Sun, Z., Habib, G.M., Lieberman, M.W., and Hannink, M. (2005). Ubiquitination of Keap1, a BTB-Kelch substrate adaptor protein for Cul3, targets Keap1 for degradation by a proteasome-independent pathway. J. Biol. Chem. *280*, 30091–30099.